


Quad-Spectral Perfect Metamaterial Absorber at Terahertz Frequency Based on a Double-Layer Stacked Resonance Structure

BEN-XIN WANG ^{1,3} QIN XIE,¹ GUANGXI DONG,¹
and WEI-QING HUANG²

1.—School of Science, Jiangnan University, Wuxi 214122, China. 2.—School of Physics and Electronics, Hunan University, Changsha 410082, China. 3.—e-mail: wangbenxin@jiangnan.edu.cn

Development of multispectral perfect light absorbers for applications in biological sensing, spectroscopic imaging, and selective thermal emitters is urgently required. Unfortunately, current multispectral absorbers are typically only based on a combination of fundamental resonances of multiple resonators using the design concepts of a coplanar superunit structure or multiple vertically stacked layers, which does not introduce new resonances while such structures are difficult to fabricate. In this work, a type of quad-spectral absorber formed by a double-layer stacked resonant structure is presented and demonstrated. Numerical simulations show that the suggested structure can achieve near 100% absorption at four frequency bands. The quad-spectral absorption results from excitation of two sets consisting of the fundamental mode and third-order resonance of the designed structure. The suggested device is insensitive to the polarization of the incident light due to the high degree of symmetry of the resonance structure. Device parameters are investigated to further explore the physical origin of the quad-spectral absorption. Moreover, it is revealed that the number of resonance peaks can be further increased by employing one more layer.

Key words: Metamaterials, terahertz, multispectral absorption

INTRODUCTION

During the past decade, metamaterials have attracted extensive attention because of their intriguing properties and potential applications. Various kinds of metamaterial-based resonance devices have also been extensively suggested and presented.^{1–4} Metamaterial-based absorbers have attracted interest for use in these resonance devices, because of their ability to achieve near 100% absorption in a thin dielectric layer with thickness much smaller than one-quarter of the resonance wavelength.⁵ Based on these resonance features including strong light absorption in an ultrathin

dielectric, metamaterial absorbers have received considerable attention.^{6–10} Unfortunately, these absorbers only show perfect absorption at a single frequency (i.e., single-spectral absorption), which is unfavorable for many applications.

To address this disadvantage of single-spectral absorption, various types of improvements have been suggested to make dual- or triple-spectral metamaterial absorbers.^{11–22} Moreover, broadband spectral absorbers have also been demonstrated by some research groups.^{23–26} Although such multispectral and broadband spectral absorbers are very desirable, the operating frequency and absorption strength of devices suggested to date are typically fixed (or unchanged), hampering their practical applications. Therefore, work on frequency- or amplitude-tunable absorbers has also attracted

much attention, and many such tunable absorbers have been reported.^{27–31}

In fact, for many applications, such as biological sensing, spectroscopic imaging, and selective thermal emitters, multispectral absorbers are required. However, unlike dual-spectral and triple-spectral absorbers that have been widely demonstrated, quad-spectral absorbers have received little attention. Very recently, several attempts to obtain quad-spectral absorbers using different design concepts have been presented; For example, some superunit coplanar structures formed by four (or more) resonators were designed to achieve quad-spectral absorption.^{32–35} Stacked resonance structures that exhibit quad-spectral or broadband-spectral absorption have been presented.^{36–39} However, these suggested quad-spectral absorbers suffer from various shortcomings. Firstly, the design concept of the superunit coplanar structure suffers from the issues of the large dimension of the unit cell and the strong interaction between the resonators, which does not follow current design trends towards miniaturization and simplification. Secondly, the design strategy for such stacked structures with four or five layers faces technical difficulties in manufacturing. Most importantly, the resonance mechanism of these suggested quad-spectral absorbers usually only involves overlapping the fundamental mode resonances of different-sized resonators, without a novel operating mechanism. Therefore, research on novel, simple designs for easy-to-fabricate quad-spectral absorbers is essential.^{38,39}

In the work presented herein, a new type of quad-spectral perfect absorber formed by only a double-layer stacked unit structure was investigated and studied. Simulation results prove that the suggested structure exhibits four separated resonance peaks, all of which exhibit absorption near 100%. The operating mechanism of the quad-spectral absorption is ascribed to the overlap between two sets consisting of the fundamental resonance and third-order response of the double-layer structure. Further numerical simulations were performed to investigate the optical properties of the design, showing that the number of resonance peaks can be further increased by employing one more layer. The proposed multispectral absorbers are promising

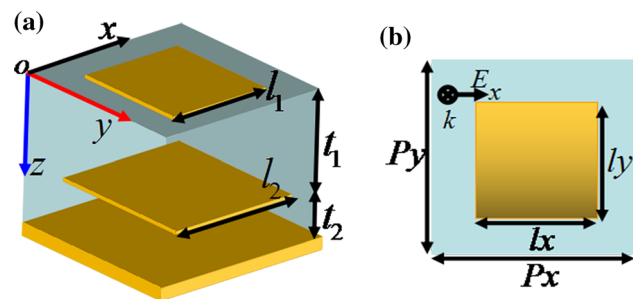


Fig. 1. (a) Three-dimensional unit cell of the quad-spectral absorber; (b) Top view of the three-dimensional unit cell of the quad-spectral absorber.

candidates for use in applications such as spectroscopic imaging, biological sensing, selective thermal emitters, and even stealth technology.

DESIGN OF UNIT CELL

Figure 1a shows the three-dimensional unit cell of the quad-spectral absorber, which is formed by two layers of square gold patches (with different lengths) and insulator dielectric slabs backed with a gold substrate. Figure 1b shows a top view of the quad-spectral absorber. The parameters of the unit cell are marked in Fig. 1. The periodicity of the unit cell is $P = P_x = P_y = 65 \mu\text{m}$. The patch lengths are $l_1 = l_{1x} = l_{1y} = 50 \mu\text{m}$, $l_2 = l_{2x} = l_{2y} = 61 \mu\text{m}$. The thickness of the gold is $0.4 \mu\text{m}$ with frequency-independent conductivity of $4.09 \times 10^7 \text{ S/m}$. The thicknesses of the insulator dielectric slab are $t_1 = 7 \mu\text{m}$ and $t_2 = 3 \mu\text{m}$, respectively, and its dielectric constant is $3(1 + i0.06)$.^{40,41} The calculation results are obtained based on finite-difference time-domain simulations (FDTD Solutions, Lumerical, Canada). In the simulations, the periodic structures are illuminated by a normally incident plane wave with electric field parallel to the x axis, perfectly matched layers are applied along the z direction, and periodic boundary conditions in the x and y directions. According to the law of conservation of energy, the suggested device obeys the following equation: $A = 1 - T - R$, where A , T , and R are the absorption, transmission, and reflection of the structure, respectively. T can be very close to zero because the thickness of the gold substrate is larger than its skin depth, while at the same time R can be suppressed when the impedance of the device matches that of air. As a result, near 100% absorption A can be achieved.

RESULTS AND DISCUSSION

The simulated absorption spectra of the multispectral absorber are shown in Fig. 2, revealing that the suggested device exhibits four resonance peaks at frequencies of $f_1 = 1.14 \text{ THz}$, $f_2 = 1.47 \text{ THz}$,

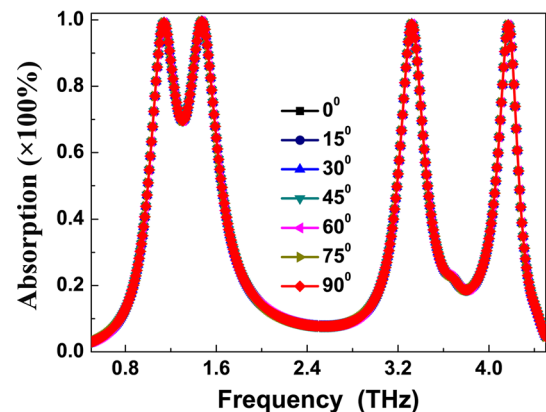


Fig. 2. Simulated absorption curve of suggested quad-spectral absorber under different polarization angles.

$f_3 = 3.32$ THz, and $f_4 = 4.17$ THz with absorptivity of 99.18%, 99.53%, 98.75%, and 98.47%, respectively. Owing to the high degree of symmetry of the dual-layer square patch structure, the suggested quad-spectral absorber is not sensitive to the polarization angle of the incident beam (Fig. 2).

The first two absorption bands f_1 and f_2 of the quad-spectral absorber derive respectively from the fundamental resonances of the two different dimensions of the square patch resonators l_1 and l_2 , while the last two resonance peaks f_3 and f_4 are ascribed to the third-order responses of the two square patches l_1 and l_2 , respectively. In other words, the combinations of two sets of the fundamental mode and third-order response of the two square patch resonator give rise to the quad-spectral absorption. According to the *LC* circuit model and classical square patch antenna theory, the resonance frequency of the metamaterial absorbers is given by⁴²

$$f_{mn} = \frac{c}{2l\sqrt{\epsilon}} \sqrt{n^2 + m^2}, \quad (1)$$

where c is the speed of light in vacuum, l is the square patch length, and ϵ is the dielectric constant of the dielectric slab. $m, n = 0, 1, 2 \dots$ are integers. According to this equation, the resonance frequency of the absorber moves to higher frequency when the length l of the square patch is decreased, thus the operating frequency of the device and the length of the metallic patch are inversely related. In particular, the operating frequency of the third-order ($m = 0$ and $n = 3$) response should be about three times that of the fundamental resonance ($m = 0$ and $n = 1$). As shown in Fig. 2, the resonance frequencies of the modes f_3 at 3.32 THz and f_4 at 4.17 THz are about three times that of the modes f_1 at 1.14 THz and f_2 at 1.47 THz, respectively. Therefore, the modes f_1 and f_2 should be the fundamental resonances of the longer and shorter patches, respectively, while the modes f_3 and f_4 should be respectively the third-order responses of the longer and shorter patches. The slight difference in the resonance frequencies is due to the weak coupling between neighboring unit cells and the different layers of the unit cell, and these weak interactions can be seen clearly in the distributions of the magnetic field in Fig. 3.

The physical picture of the multispectral absorption can be better understood by analyzing the magnetic field ($|H_y|$) distributions of these resonance modes. Figure 3 shows the $|H_y|$ field distributions of the four absorption peaks. It can be seen that the $|H_y|$ field distributions for the four absorption maximums are chiefly focused on the insulator dielectric slabs of the quad-spectral absorber. As a result, the four absorption modes f_1, f_2, f_3 , and f_4 can all be attributed to the localized resonance responses of the suggested device. Furthermore, for the absorption peak at 1.14 THz (f_1), there is only one strong node in the distribution of the

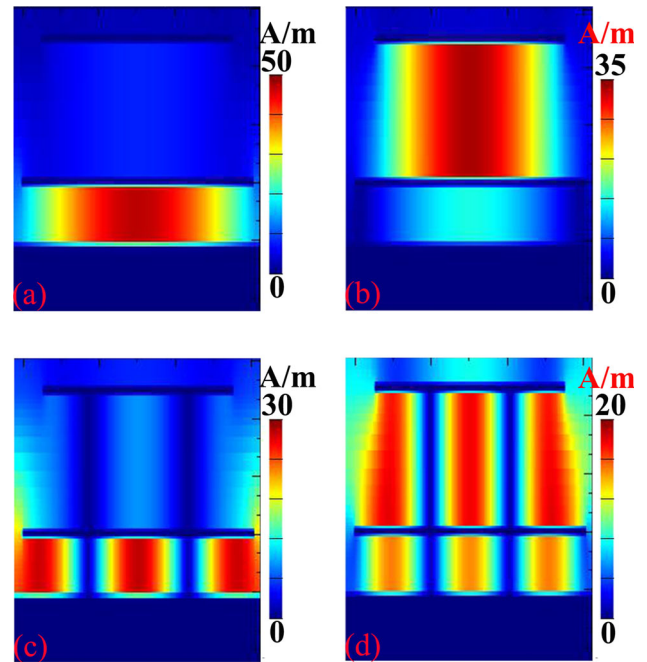


Fig. 3. (a, b) Distributions of magnetic field ($|H_y|$) for the resonance modes f_1 and f_2 of the quad-spectral absorber, respectively. (c, d) Distributions of magnetic field ($|H_y|$) for the resonance modes f_3 and f_4 of the quad-spectral absorber, respectively.

magnetic field in dielectric slab t_2 (Fig. 3a). For the absorption peak at 3.32 THz (f_3), three strong nodes in the distribution of the magnetic field in dielectric slab t_2 can be observed (Fig. 3c). Therefore, the resonance modes f_1 and f_3 are the fundamental resonance and third-order response of the longer square patch l_2 , respectively.^{43–46} Similarly, for the resonance modes f_2 and f_4 , it is found that their $|H_y|$ field distributions are mostly focused on dielectric slab t_1 , while only a small section of the field distributions can be observed in dielectric slab t_2 (Fig. 3b, d). In particular, for the absorption peak at 1.47 THz (f_2), the $|H_y|$ field (Fig. 3b) shows only one node in dielectric slab t_1 , while there are three strong nodes in dielectric slab t_1 for the absorption peak at 4.17 THz (f_4) (Fig. 3d). According to these field distribution features, modes f_2 and f_4 are the fundamental resonance and third-order response of the shorter square patch l_1 . Obviously, the overlap between two sets of the fundamental resonance and third-order response of the two square patch resonators of different sizes gives rise to the quad-spectral absorption. This kind of operating mechanism represents a new way to decrease the number of resonators (and thus simplify the design of the structure), because the combined effects of the fundamental resonance and third-order response of the metamaterial design are utilized, which is different from previously reported designs in which many resonators (at least as many as the number of absorption peaks) are required, because they only

employ the fundamental resonance of the unit structure.^{32–38}

The suggested quad-spectral absorber is insensitive to the polarization of the incident radiation because of the high degree of symmetry of the square patch resonators. However, for some applications, an absorber that is polarization switchable instead of insensitive to the polarization angle can be used for frequency tuning. According to Eq. 1, the resonance frequency of the absorber device is inversely proportional to the square patch length. Therefore, a quad-spectral polarization-controllable perfect light absorber can be simply obtained by varying the sizes of the metallic patches in two orthogonal directions. Here, we only change the lengths of the metallic patches in the y -direction as an example, i.e., $l_{1y} = 47 \mu\text{m}$ and $l_{2y} = 58 \mu\text{m}$, with other structural parameters remaining unchanged. Figure 4a shows the calculated absorption spectra in 0° (along x -direction) and 90° (along y -direction) for the designed device, revealing that the suggested device is sensitive to the polarization angle of the incident beam. The polarization-tunable multi-spectral absorber has potential applications in

detecting waves with specific polarization and the fingerprints of some explosive materials.

We next investigate the influence of the thicknesses of the insulator dielectric slabs on the performance of the quad-spectral absorption. Figure 4b and c show the dependence of the absorption spectra on the thickness of the insulator dielectric slabs t_1 and t_2 , respectively. As revealed in Fig. 4b, changing the thickness of insulator dielectric slab t_1 chiefly influences the frequencies of the modes f_2 and f_4 , consistent with the theoretical description above indicating that the modes f_2 and f_4 are the fundamental mode and third-order resonance of the longer patch l_1 (or the $|H_y|$ field distributions of the two modes are mostly focused on this dielectric slab; Fig. 3b, d). Similarly, when changing the thickness of insulator dielectric slab t_2 , the frequencies of the resonance modes f_1 and f_3 gradually increase with decrease of t_2 , while the frequency changes of the modes f_2 and f_4 are negligible (Fig. 4c).

The number of spectral bands can be further increased by stacking one more layer (i.e., changing the original two-layer structure to a three-layer structure). The optimal thicknesses of the insulator

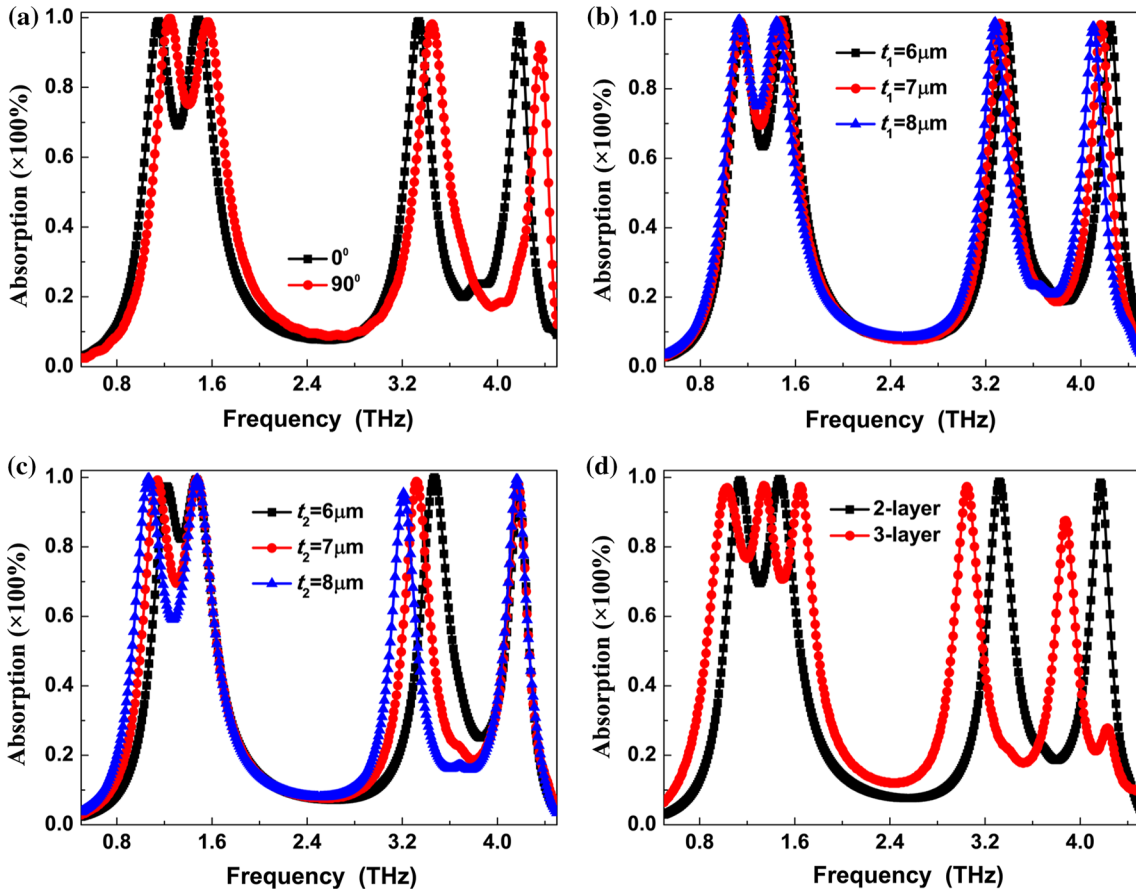


Fig. 4. (a) Calculated absorption spectra in 0° (electric field along the x -direction) and 90° (electric field along the y -direction) of the polarization-controllable absorber; (b, c) dependence of the absorption spectra on the thickness of the dielectric layers t_1 and t_2 of the polarization-insensitive absorber, respectively; (d) dependence of the absorption spectra on the stacking layer of the multispectral absorber.

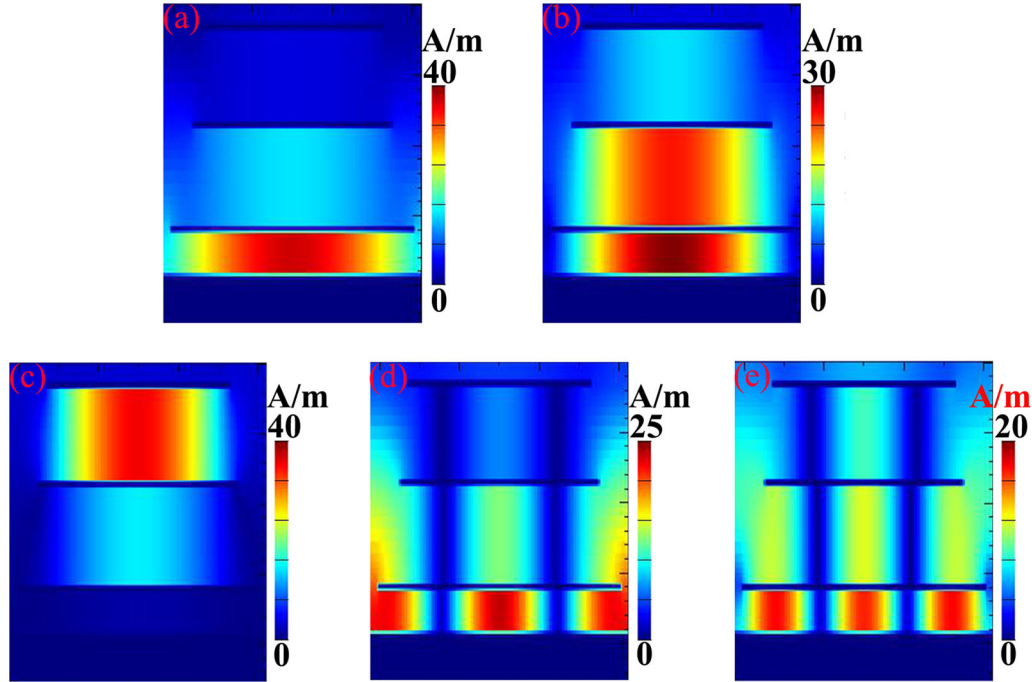


Fig. 5. Distributions of the magnetic field ($|H_y|$) for the resonance modes (a) f_1 , (b) f_2 , (c) f_3 , (d) f_4 , and (e) f_5 of the penta-spectral absorber, respectively.

dielectric slab in the three-layer structure are $t_1 = 7 \mu\text{m}$, $t_2 = 7 \mu\text{m}$, and $t_3 = 3 \mu\text{m}$ (from the top to bottom layer), and the lengths of the square patch are $l_1 = 46 \mu\text{m}$, $l_1 = 50 \mu\text{m}$, and $l_1 = 61 \mu\text{m}$ (also from the top to bottom layer). The periodicity of the unit cell and the dielectric constant of the insulator dielectric slab are unchanged. Figure 4d shows the dependence of the absorption spectra on the stacking layer of the suggested absorber. As given, the three-layer structure enables five discrete absorption peaks located at around $f_1 = 1.03 \text{ THz}$, $f_2 = 1.34 \text{ THz}$, $f_3 = 1.65 \text{ THz}$, $f_4 = 3.05 \text{ THz}$, and $f_5 = 3.88 \text{ THz}$, respectively. To better explore the operating mechanism of the penta-spectral absorber, the distributions of the magnetic field $|H_y|$ corresponding to the five different resonance bands are presented in Fig. 5. These results show that the five different resonance modes can all be ascribed to the localized resonance responses of the suggested three-layer structure, because their $|H_y|$ field are all focused on the insulator dielectric slab of the penta-spectral absorber. According to the distributions of the magnetic field in the insulator dielectric slab, it is clear that the first three resonance modes f_1 , f_2 , and f_3 are due to the coupling effects of the fundamental resonances in patches of different sizes (Fig. 5a–c), while the last two modes f_4 , and f_5 should be due to hybridization effects of the three-order responses of the patches (Fig. 5d, e).

CONCLUSIONS

We present a quad-spectral terahertz absorber consisting of two alternating layers of square gold patches and insulator dielectric slabs backed with a

gold substrate. Four spectral bands with near 100% absorption are obtained. The physical mechanism of the quad-spectral absorption is caused by the overlapping of two sets of the fundamental resonance and three-order response of the square gold patch resonator. The multispectral absorption is explored by analyzing the distributions of the magnetic field at the four spectral bands. Furthermore, a quad-spectral polarization-controllable absorber can be realized by merely reshaping the sizes of the gold patches in two orthogonal directions, while the design can be modified to a penta-spectral terahertz absorber by adding one more gold patch layer. The suggested multispectral absorbers are promising candidates for detection of the fingerprints of some explosive materials, as well as in spectroscopic imaging and detectors.

ACKNOWLEDGMENTS

This work was supported by the National Natural Science Foundation of China (Grant No. 11647143), Natural Science Foundation of Jiangsu Province (Grant No. BK20160189), and the Fundamental Research Funds for the Central Universities (Grant No. JUSRP51721B).

REFERENCES

1. S. Zhang, D.A. Genov, Y. Wang, M. Liu, and X. Zhang, *Phys. Rev. Lett.* 101, 047401 (2008).
2. B. Lukyanchuk, N.I. Zheludev, S.A. Maier, N. Halas, J.P. Nordlander, H. Giessen, and C.T. Chong, *Nat. Mater.* 9, 707 (2010).
3. Y.S. Lin, Y. Qian, F. Ma, Z. Liu, P. Kropelnicki, and C. Lee, *Appl. Phys. Lett.* 102, 111908 (2013).

4. L. Cong, W. Cao, X. Zhang, Z. Tian, J. Gu, R. Singh, J. Han, and W. Zhang, *Appl. Phys. Lett.* 103, 171107 (2013).
5. N.I. Landy, S. Sajuyigbe, J.J. Mock, D.R. Smith, and W.J. Padilla, *Phys. Rev. Lett.* 100, 207402 (2008).
6. J. Zhao, X. Huang, and H. Yang, *Appl. Phys. A* 122, 487 (2016).
7. G.M. Akselrod, J. Huang, T.B. Hoang, P.T. Bowen, L. Su, D.R. Smith, and M.H. Mikkelsen, *Adv. Mater.* 27, 8028 (2015).
8. L. Cong, S. Tan, R. Yahiaoui, F. Yan, W. Zhang, and R. Singh, *Appl. Phys. Lett.* 106, 031107 (2015).
9. F. Zhang, S. Feng, K. Qiu, Z. Liu, Y. Fan, W. Zhang, Q. Zhao, and J. Zhou, *Appl. Phys. Lett.* 106, 091907 (2015).
10. R. Walter, A. Till, A. Berrier, F. Sterl, T. Weiss, and H. Giessen, *Adv. Opt. Mater.* 3, 398 (2015).
11. P. Rufangura and C. Sabah, *J. Alloys Compd.* 671, 43 (2016).
12. H. Xiong, L.L. Zhong, C.M. Luo, and J.S. Hong, *AIP Adv.* 5, 067162 (2015).
13. G. Yao, F. Ling, J. Yue, C. Luo, J. Ji, and J. Yao, *Opt. Express* 24, 1518 (2015).
14. X. Liu, C. Lan, K. Bi, B. Li, Q. Zhao, and J. Zhou, *Appl. Phys. Lett.* 109, 062902 (2016).
15. B.X. Wang, G.Z. Wang, and L.L. Wang, *Plasmonics* 11, 523 (2016).
16. M. Zhong, G.M. Han, S.J. Liu, B.L. Xu, J. Wang, and H.Q. Huang, *Phys. E* 86, 158 (2017).
17. B.X. Wang, X. Zhai, G.Z. Wang, W.Q. Huang, and L.L. Wang, *J. Appl. Phys.* 117, 014504 (2015).
18. X. Shen, Y. Yang, Y. Zang, J. Gu, J. Han, W. Zhang, and T.J. Cui, *Appl. Phys. Lett.* 101, 154102 (2012).
19. B.X. Wang, *IEEE J. Select. Top. Quantum Electron.* 23, 4700107 (2017).
20. B. Lin, S. Zhao, X. Da, Y. Fang, J. Ma, W. Li, and Z. Zhu, *J. Appl. Phys.* 117, 184503 (2015).
21. J. Chen, Z. Hu, S. Wang, X. Huang, and M. Liu, *Eur. Phys. J. B* 89, 14 (2016).
22. S. Shang, S. Yang, L. Tao, L. Yang, and H. Cao, *AIP Adv.* 6, 075203 (2016).
23. P. Rufangura and C. Sabah, *J. Alloys Compd.* 680, 473 (2016).
24. J. Tang, Z. Xiao, K. Xu, X. Ma, and Z. Wang, *Plasmonics* 11, 1393 (2016).
25. X. Huang, X. He, L. Guo, Y. Yi, B. Xiao, and H. Yang, *J. Opt.* 17, 055101 (2015).
26. V.A.L. Mol and C.K. Aanandan, *J. Phys. Commun.* 1, 015003 (2017).
27. P. Pitchappa, C.P. Ho, P. Kropelnicki, N. Singh, D.L. Kwong, and C.K. Lee, *J. Appl. Phys.* 104, 201114 (2014).
28. M.K. Hedayati, A.U. Zilohu, T. Strunskus, F. Faupel, and M. Elbahri, *Appl. Phys. Lett.* 104, 041103 (2014).
29. Y. Huang, G. Wen, W. Zhu, J. Li, L.-M. Si, and M. Premaratne, *Opt. Express* 22, 16408 (2014).
30. G. Isic, B. Vasic, D.C. Zografopoulos, R. Beccherelli, and R. Gajic, *Phys. Rev. Appl.* 3, 064007 (2014).
31. P. Pitchappa, C.P. Ho, Y.-S. Lin, P. Kropelnicki, C.-Y. Huang, N. Singh, and C. Lee, *Appl. Phys. Lett.* 104, 151104 (2014).
32. D. Xiao and K. Tao, *Appl. Phys. Express* 8, 102001 (2015).
33. W. Agarwal, A.K. Behera, and M.K. Meshram, *Electron. Lett.* 52, 340 (2016).
34. D.T. Viet, N.T. Hien, P.V. Tuong, N.Q. Minh, P.T. Trang, L.N. Le, Y.P. Lee, and V.D. Lam, *Opt. Commun.* 322, 209 (2014).
35. J.W. Park, P.V. Tuong, J.Y. Rhee, K.W. Kim, W.H. Jang, E.H. Choi, L.Y. Chen, and Y.P. Lee, *Opt. Express* 21, 9691 (2013).
36. G. Dayal and S.A. Ramakrishna, *J. Opt.* 15, 055106 (2013).
37. H. Luo, X. Hu, Y. Qiu, and P. Zhou, *Solid State Commun.* 188, 5 (2014).
38. S. Liu, H. Chen, and T.J. Cui, *Appl. Phys. Lett.* 106, 151601 (2015).
39. S. Liu, J. Zhuge, S. Ma, H. Chen, D. Bao, Q. He, L. Zhou, and T.J. Cui, *J. Appl. Phys.* 118, 245304 (2015).
40. L. Huang, D.R. Chowdhury, S. Ramani, M.T. Reiten, S.N. Luo, A.K. Azad, A.J. Taylor, and H.T. Chen, *Appl. Phys. Lett.* 101, 101102 (2012).
41. N.K. Grady, J.E. Heyes, D.R. Chowdhury, Y. Zeng, M.T. Reiten, A.K. Azad, A.J. Taylor, D.A.R. Dalvit, and H.T. Chen, *Science* 340, 6138 (2013).
42. X.Y. Peng, B. Wang, S. Lai, D.H. Zhang, and J.H. Teng, *Opt. Express* 20, 27756 (2012).
43. G. Dayal and S.A. Ramakrishna, *J. Opt.* 16, 094016 (2014).
44. B.X. Wang, G.Z. Wang, T. Sang, and L.L. Wang, *Sci. Rep.* 7, 41373 (2017).
45. G. Dayal and S.A. Ramakrishna, *J. Phys. D* 48, 035105 (2015).
46. B.X. Wang, *Plasmonics* 12, 95 (2017).

Publisher's Note Springer Nature remains neutral with regard to jurisdictional claims in published maps and institutional affiliations.